Constitutive behavior of AA5383 alloy at high temperature deformation

R. DU[a], C. MAREAU[a], Y. AYED[a], P. D. SANTO[a]

a. LAMPA, ENSAM, 2 boulevard du Ronceray, 49035 Angers, Cedex 01 - France
rou.du@ensam.eu, charles.mareau@ensam.eu, yessine.ayed@ensam.eu,
philippe.dalsanto@ensam.eu

Abstract:

In this study, the behavior of a 5383 aluminum alloy is investigated. An experimental campaign, including uniaxial tension and free bulging tests, is performed to characterize the mechanical properties. The BBC2003 yield criterion with a composite hardening model is employed to describe the constitutive behavior. The model is implemented in the ABAQUS finite element solver with a user subroutine. The identified model is validated by comparing numerical and experimental results obtained for the hot forming of a complex shape specimen at 673 K and 0.001 s^{-1}. The experimental and numerical results (strain field and thickness distribution) are in good agreement.

Keywords: AA5383 alloy, BBC2003 yield function, gas forming

1 Introduction

Aluminum alloys with magnesium as the major alloying element are widely used in the automotive and marine industries due to their corrosion resistance, high strength to weight ratio and important ductility. For marine applications, the most commonly used wrought aluminum alloys are 5083/5383 alloys. Many efforts have been made to investigate the impact of welding on mechanical properties of AA5383 alloy [1]. However, little attention has been given to the constitutive behavior of this alloy, especially at high temperatures, though this aspect is very important for its further application in the automotive and marine industry.

An appropriate description of the material behavior is essential to obtain reliable results. For this purpose, constitutive equations must include the influence of temperature and strain rate on the flow behavior. Those equations can be categorized into physics-based models and phenomenological models. Physics-based models often use thermodynamics and kinetics of crystallographic slip to relate flow stress, strain rate and temperature [2, 3]. They can be formulated at the slip system level or directly at the macroscopic scale. On the other hand, phenomenological models directly describe the effect of strain hardening, strain rate and temperature on the deformation behavior. Phenomenological models can be formulated in either the separated or the integrated form. When the separated form is used, the influence of strain hardening, strain rate sensitivity and temperature softening on the flow resistance is independent. Such models can be constructed in additive or multiplicative manners [4]. For integrated phenomenological models, variables are not separated which allows considering more complex mechanisms such as temperature-dependent strain hardening [4] and rate-dependent strain hardening [5]. A partial review of phenomenological models can be found in Sun et al. [4]. Phenomenological models are more widely used than physics-based models due to their ease of identification and implementation.

This study aims at proposing a constitutive model to predict the high temperature deformation behavior the AA5383 alloy under plane stress conditions. For this purpose, uniaxial tension tests are performed at different strain rates (10^{-4}-10^{-1} s^{-1}) and temperatures (623-723 K). A composite hardening model with BBC2003 yield criterion is proposed and identified. Simulation and experiment are carried out on gas forming with complex axisymmetric shape die. The surface principal logarithmic strain and thickness evolution predicted by the finite element analysis are compared to the experimental results.

2 Experimental study

2.1 Material and specimen geometry

The present study focuses on the 5383 aluminum alloy, whose chemical composition is given in Table 1. The studied alloy has been rolled to obtain 3.2 mm thick sheets that have been heat treated at 623 K for 5 min to increase the ductility. The corresponding microstructure is shown in Fig. 1. It is composed of equiaxed grains with an average size of 19 µm.

Table 1
Chemical composition of AA5383 alloy

Material	Mg(%)	Mn(%)	Fe(%)	Cr(%)	Si(%)	Cr(%)	Cu	Zn	Al
AA5383	4.91	0.80	0.17	0.12	0.05	0.12	0.06	0.04	balance

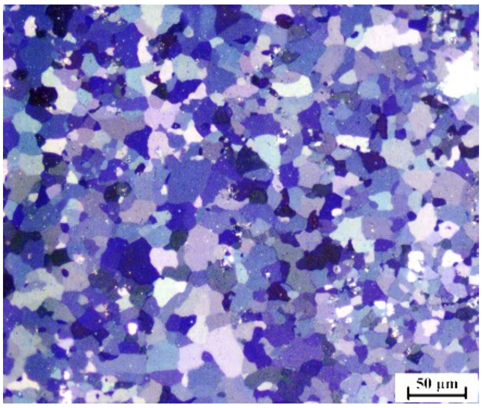

Fig. 1. Microstructure of AA5383 alloy sheet after heat treatment at 623 K for 5 min

In order to characterize the material properties, two types of specimens have been machined: Uniaxial Tension (UT) specimens with a 78.14 mm long and 12.5 mm wide gauge section and Free Bulging (FB) flanges of 290 mm diameter. The UT tests are performed on a GLEEBLE 3500 machine while the FB tests are carried out on a gas forming machine (shown in Fig. 2). The testing conditions are for UT specimens are listed in Table 2. The FB tests have been performed under three constant pressures (0.6, 1.0 and 1.5 MPa). The anisotropic properties of our material is assumed not to be influenced by temperature and strain rate in the studied range. The characterization of anisotropy is fixed at 673 K and 0.001 s^{-1}.

Table 2
Testing conditions for UT specimens (Degree is the degree along the rolling direction; T and $\dot{\varepsilon}$ are temperature and strain rate, respectively)

T \ $\dot{\varepsilon}$ \ Degree	0.0001 s^{-1}	0.001 s^{-1}	0.01 s^{-1}	0.1 s^{-1}
623 K	0°	0°	0°	0°
673 K	0°	0°, 45° and 90°	0°	0°
723 K	0°	0°	0°	0°

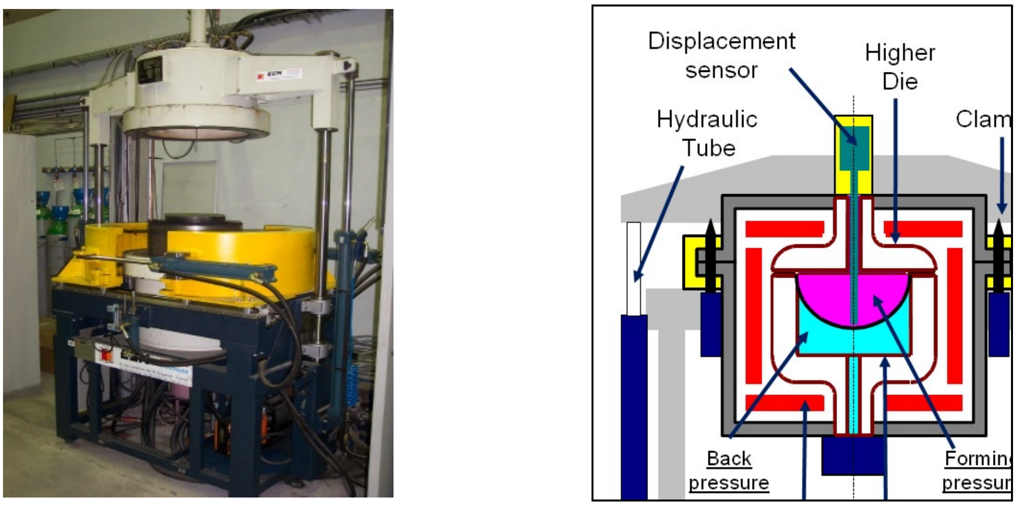

(a) (b)
Fig. 2. (a) Gas forming machine at LAMPA and (b) pressure scheme

2.2 Results

The true axial stress-strain curves at different temperatures and strain rates obtained from the UT tests along the rolling direction are shown in Fig. 3. The influence of temperature and strain rate on the flow resistance behavior is significant. Generally, both the yield stress and the steady stress increase with an increasing strain rate and a decreasing temperature. A yield drop phenomenon, which is particularly visible for high strain rates, is sometimes observed. This phenomenon can be explained by the sudden increase of the dislocation density at the beginning of deformation. Also, whatever the deformation temperature is, a hardening behavior is observed at low strain rates while softening is predominant for high strain rates.

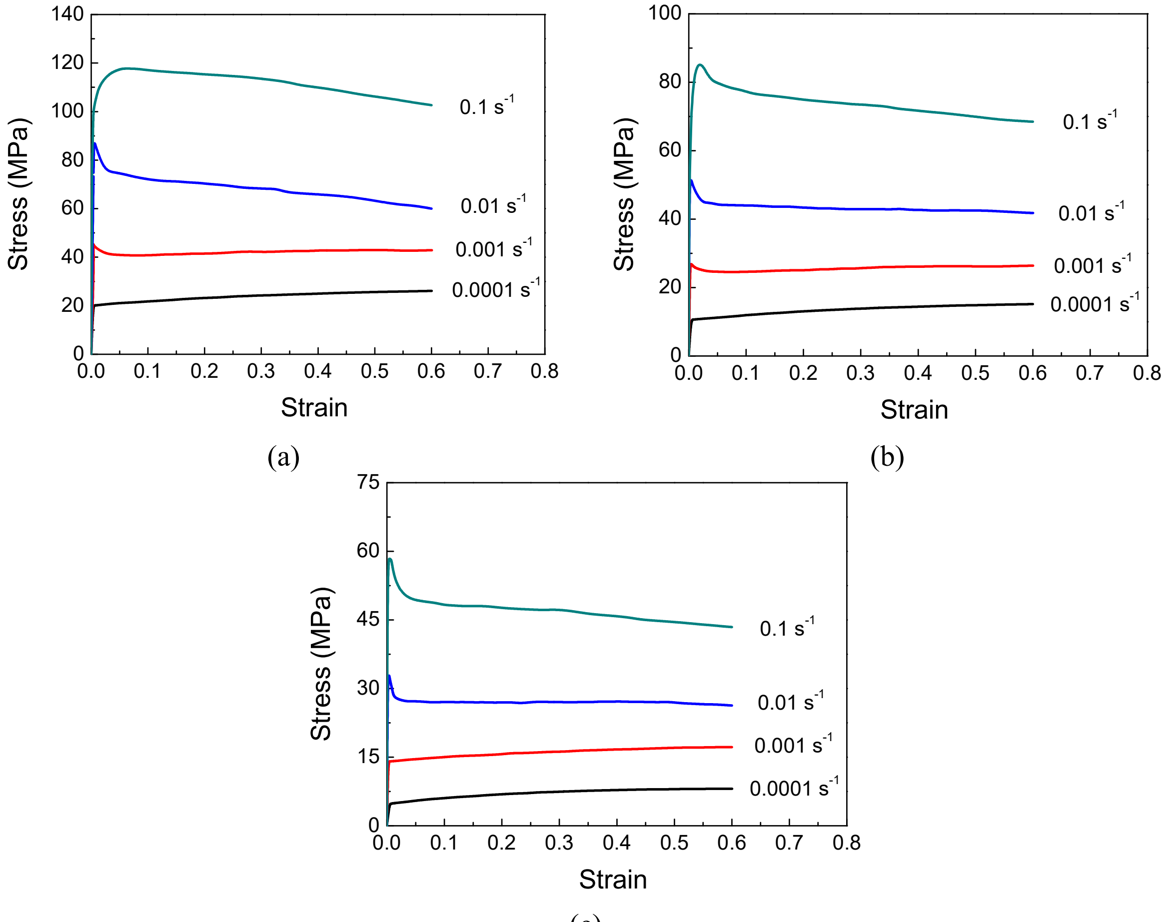

Fig. 3. Stress-strain curves for UT tests along the rolling direction at (a) 623 K; (b) 673 K and (c) 723 K

The stress-strain curves obtained for different loading directions (i.e. 0°, 45° and 90°) at 673 K and 0.001 s^{-1} are plotted in Fig. 4. According to the results, the material exhibits a small degree of plastic anisotropy. The flow stress is the highest for the rolling direction and the lowest for the intermediate direction. The corresponding Lankford coefficients are lower than unity, with r_0 = 0.71, r_{45} = 0.88 and r_{90} = 0.78. The experimental data for r-values are very close to the values of Al-Mg alloys at elevated temperatures given in Ref. [6].

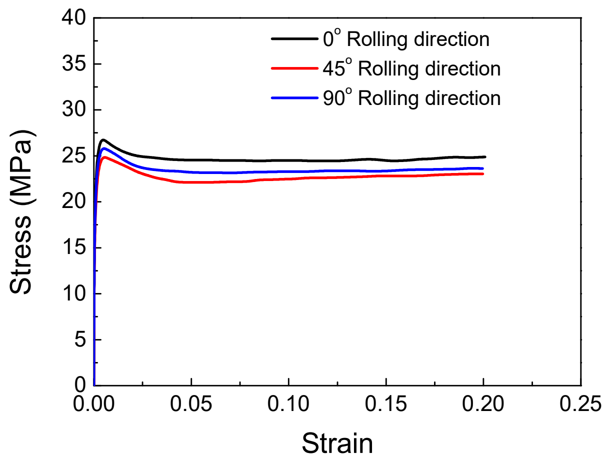

Fig. 4. Stress-strain curves for UT tests in different rolling directions at 673 K and 0.001 s^{-1}

The evolution of the dome height with respect to time for FB tests under three different constant forming pressures is presented in Fig. 5. All the tests have been stopped at a dome displacement of 70 mm. It can be seen that the displacement rate is not linearly related to the pressure value. The dome height grows rapidly at the beginning of the test before reaching a steady state where the displacement rate is constant. To the same extent of deformation, the highest pressure allows reducing the forming time significantly.

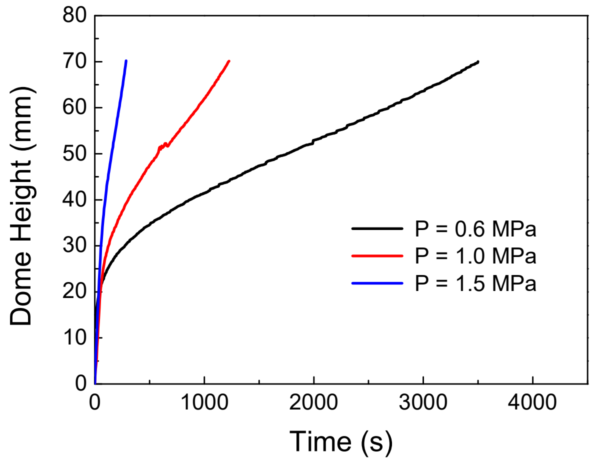

Fig. 5. Dome height evolution for FB tests under three constant pressures

3 Constitutive equations

The presented numerical approach must be able to accurately predict the flow behavior of the AA5383 alloy submitted to hot forming conditions. The proposed material model focuses on temperature and strain rate dependent plasticity. The main constitutive equations associated to this approach are introduced in this section.

The yield function is given by

$$\Phi(\sigma_{ij},\bar{\varepsilon}_p,\dot{\bar{\varepsilon}}_p,T)=\bar{\sigma}(\sigma_{ij})-Y_{ref}[\bar{\varepsilon}_p,\dot{\bar{\varepsilon}}_p,T]=0 \tag{1}$$

where Y_{ref} is the deformation resistance depending on the equivalent plastic strain $\bar{\varepsilon}_p$, the equivalent plastic strain rate $\dot{\bar{\varepsilon}}_p$ and the temperature T. In our study, the BBC2003 yield criterion is used and the equivalent stress $\bar{\sigma}$ is given by

$$\bar{\sigma}=[a(\Gamma+\Psi)^{2k}+a(\Gamma-\Psi)^{2k}+(1-a)(2\Lambda)^{2k}]^{\frac{1}{2k}} \tag{2}$$

where k and a are material parameters. The yield locus is convex for $k\in N\geq 1$, $0\leq a\leq 1$, respectively. Γ, Ψ and Λ are functions which are given by

$$\Gamma=\frac{\sigma_{11}+M\sigma_{22}}{2}$$
$$\Psi=\sqrt{\frac{(N\sigma_{11}-P\sigma_{22})^2}{4}+Q^2\sigma_{12}\sigma_{21}} \tag{3}$$
$$\Lambda=\sqrt{\frac{(R\sigma_{11}-S\sigma_{22})^2}{4}+T^2\sigma_{12}\sigma_{21}}$$

In the above two equations, a , M , N , P , Q , R , S and T are yield criterion constants. The integer parameter k is associated with the crystallographic structure of the material. The recommended value for k is 4 for FCC materials [7].

The hardening of the material is assumed to be purely isotropic and neither kinematic nor distortional hardening is considered. The hardening law is assumed to be given by

$$Y_{ref}[\bar{\varepsilon}_p] = K(\bar{\varepsilon} + \bar{\varepsilon}_0)^n \exp(-b\bar{\varepsilon}) \tag{4}$$

where K, $\bar{\varepsilon}_0$, n and b are strain hardening parameters. In close analogy with the Johnson-Cook model [8], the yield stress is assumed to be independently scaled by a temperature and a strain rate term,

$$Y_{ref}[\bar{\varepsilon}_p, \dot{\bar{\varepsilon}}_p, T] = Y[\bar{\varepsilon}_p]Y[\dot{\bar{\varepsilon}}_p]Y[T] \tag{5}$$

with

$$Y[\dot{\bar{\varepsilon}}_p] = \dot{\bar{\varepsilon}}^m \quad and \quad Y[T] = 1 - (\frac{T - T_r}{T_m - T_r})^\beta \tag{6}$$

where m is the strain-rate sensitivity parameter while the temperature parameters are: the reference temperature T_r, the melting temperature T_m, and the exponent β.

4 Parameter identification

In this section, the parameters of the constitutive model have been identified based on the UT and FB experimental results at different temperatures and strain rates.

4.1 Hardening rule parameters

A genetic algorithm has been used to obtain the parameters of the hardening rule. The reference temperature is set to T_r = 623 K. The objective function is defined in terms of the relative error between the calculated stress $\bar{\sigma}^C$ and experimental stress $\bar{\sigma}^E$:

$$f(x) = \sum \frac{\left|\bar{\sigma}^C - \bar{\sigma}^E\right|}{\bar{\sigma}^E} \tag{7}$$

where $f(x)$ is the sum of relative errors for the UT tests along the rolling direction for the different temperatures and strain rates. The detailed computation procedure can be found in [9]. Compared to traditional optimization techniques, the GA technique can overcome the difficulties associated with local minima. In this work, the population consists of 10000 individuals, the maximum number of generations is 100, the crossover probability is 0.8 and the mutation probability is 0.02. The identified parameter values are listed in Table 3.

Table 3
Material parameters for a composite model

K	$\bar{\varepsilon}_0$	n	m	b	β
480	0.82	0.65	0.24	0.60	0.28

4.2 Yield function parameters

In the conventional identification of BBC2003 yield criterion, the following experimental data are considered to be given:

- Three uniaxial yield stresses obtained from UT tests along the 0°, 45° and 90° directions (denoted here as Y_0, Y_{45} and Y_{90}).
- Three r-values corresponding to 0°, 45° and 90° orientations (denoted here as r_0, r_{45} and r_{90}).
- The biaxial yield stress (denoted here as Y_b).
- The biaxial r-value (ratio of plastic strain in transverse direction to the plastic strain in rolling direction), denoted as r_b.

In this study, the experimental coefficient of biaxial plastic anisotropy (r_b) is not available. The most convenient strategy to handle this problem is to use the following constraint $r_b = 1$. Indeed, some authors have shown that, for metallic sheets, this constraint can lead to well-shaped yield loci [10]. The value of biaxial yield stress Y_b in this configuration is not explicit. It can be obtained from free bulging tests by using an inverse method to fit the dome height evolution. The other required data have been obtained from the UT tests for different loading directions (i.e. 0°, 45° and 90°) directly. The common way to solve the anisotropy parameters is to define an error function ς by means of Gaussian square of error [10]

$$\varsigma(a,M,N,P,Q,R,S,T) = \sum_{i=1}^{3}\left(\frac{\bar{\sigma}_{\theta_i} - Y_{\theta_i}^{\exp}}{Y_{\theta_i}^{\exp}}\right)^2 + \left(\frac{\bar{\sigma}_b - Y_b^{\exp}}{Y_b^{\exp}}\right)^2 + \sum_{i=1}^{3}\left(\frac{r_{\theta_i} - r_{\theta_i}^{\exp}}{r_{\theta_i}^{\exp}}\right)^2 + \left(\frac{r_b - r_b^{\exp}}{r_b^{\exp}}\right)^2 \quad (8)$$

where $\{\theta_1, \theta_2, \theta_3\} = \{0^o, 45^o, 90^o\}$. An improved Newton Raphson method, due to the work of Banabic et al., is employed for the parameter identification [10]. The performance of this algorithm depends on the proper initial vector choice. In this study, this vector is fixed to [0.7, 1.2, 1, 1, 1, 1, 1, 1] which can ensure convergence.

The inverse method is used for analyzing free bulging tests under three constant forming pressures. The numerical model, shown in Fig. 6, is adopted to simulate the experimental forming of a spherical dome. Only a quarter part is considered due to the model symmetry (shell mesh and loading conditions). The experimental forming pressure is applied on the upper face of the sheet. The interaction between the sheet (Slave) and the die (Master) is controlled by a hard contact algorithm (surface to surface) with Coulomb friction of 0.1. Shell elements with reduced integration are chosen for the sheet mesh while the die and blank holder are defined as discrete rigid surfaces.

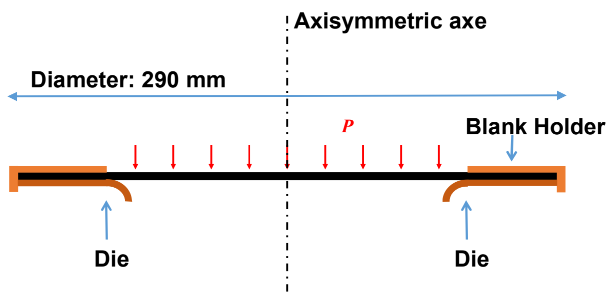

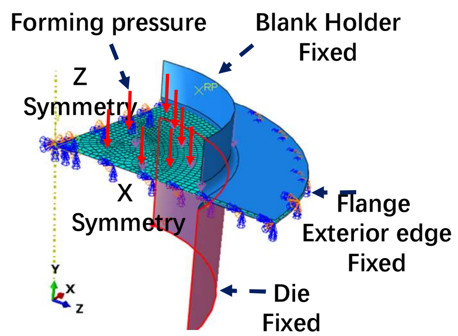

(a) (b)

Fig. 6. (a) Geometry and (b) simulation model for FB

For the inverse method, the dome height evolution is chosen as the output variables and the objective function is defined by

$$Error = \sum (h_{i,sim} - h_{i,\exp})^2 \tag{9}$$

where $h_{i,sim}$ is the simulated dome height value at the ith time and $h_{i,\exp}$ is the corresponding experimental value. The biaxial yield stress is changed iteratively to fit the simulated dome height evolutions to the experimental results. It is found that, when the biaxial yield stress is Y_b = 34.1 MPa, the numerical simulation can predict the dome height evolutions (Fig. 7). The average errors for the forming pressure of 0.6 MPa, 1.0 MPa and 1.5 MPa are 4.2%, 6.9% and 6.3%, respectively. The computed ratio between biaxial yield stress and uniaxial yield stress at 673 K and 0.001 s^{-1} is around 1.3 instead of 1.0 which is the value under the assumption of isotropy. Similar phenomenon has also been reported for the Mg AZ31 sheet alloy [11]. The parameters of the BBC2003 yield criterion are shown in Table 4.

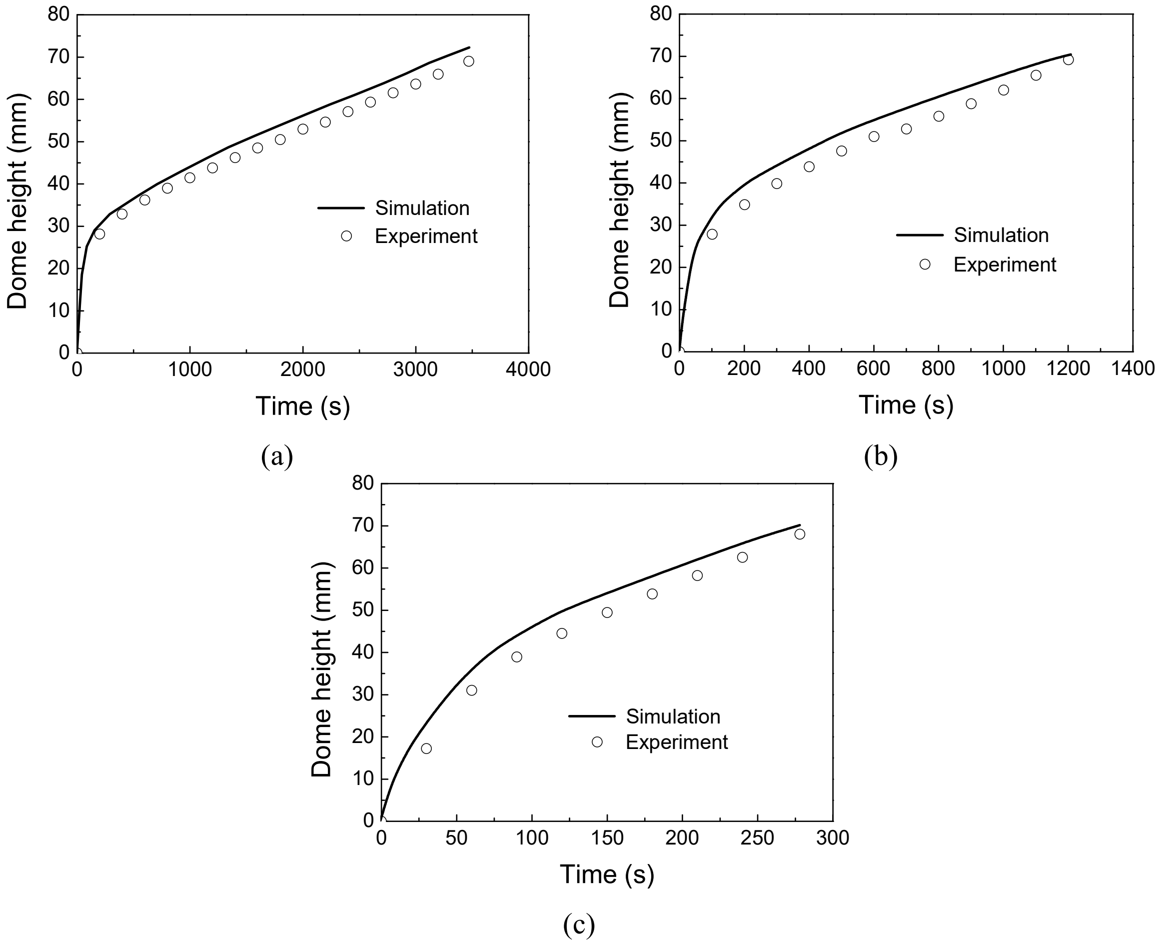

Fig. 7. Results of inverse analysis for FB: experimental data vs. numerical design for forming pressure at (a) 0.6 MPa; (b) 1.0 MPa and (c) 1.5 MPa

Table 4
BBC2003 anisotropic parameters for AA5383 alloy

a [-]	M [-]	N [-]	P [-]	Q [-]	R [-]	S [-]	T [-]	Y_{ref} [MPa]	k [-]
0.0381	1.1223	1.9355	1.9259	2.1137	0.8106	0.8604	0.8913	26.8	4

5 Validation

In order to validate the constitutive model, a forming simulation with a complex axisymmetric shape die is performed at 673 K. The applied pressure has been computed to obtain a maximum equivalent strain rate of 0.001 s^{-1}. The model conditions are similar to those used for free bulging test simulations, as shown in Fig. 8 (a)). The computed pressure law, seen in Fig. 8 (b), has been used as an input in the forming experiment.

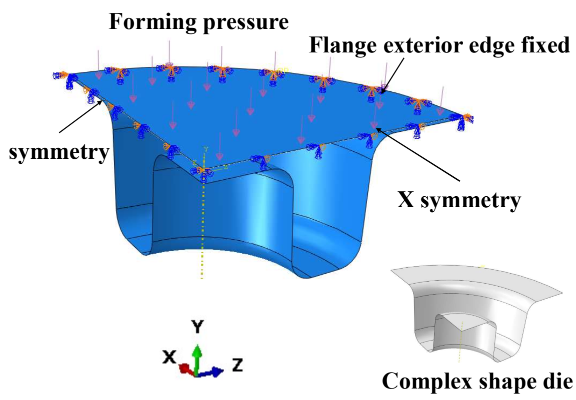

(a)

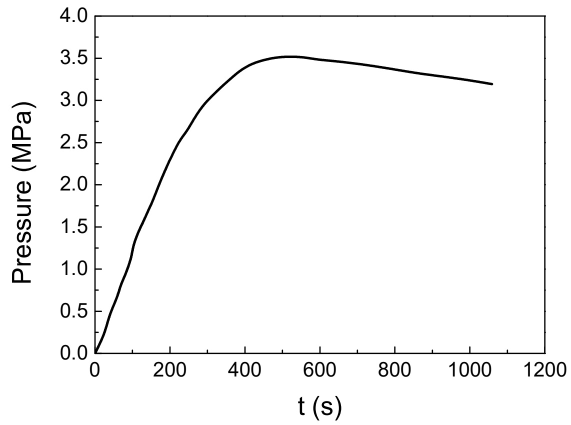

(b)

Fig. 8 Numerical model for gas forming with a complex shape die

The forming experiment is carried out on the gas forming machine (Fig. 2). With the GOM software, the maximum principal logarithmic strain of the deformed part is measured and the corresponding distribution is shown in Fig. 9 (a). The maximum strain is concentrated on the inner edge. The evolutions of the principal strain and the thickness have been plotted on a line along the rolling direction from the center to the edge. The experimental maximum value of the principal logarithmic strain is about 0.42 while the lowest thickness is 1.63 mm, which both are located 40 mm away from the center point. According to the results, the proposed constitutive model allows predicting both the maximum principal logarithmic strain and thickness. The calculated errors for the principal logarithmic strain and thickness at a 40 mm distance from the center are 4.3% and 7.9%, respectively.

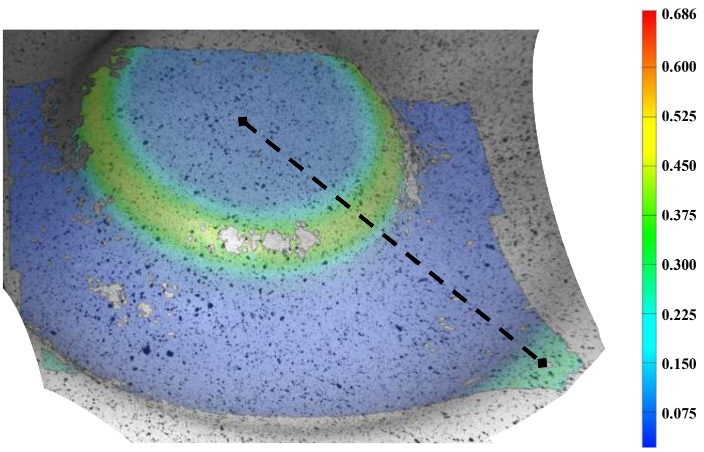

(a)

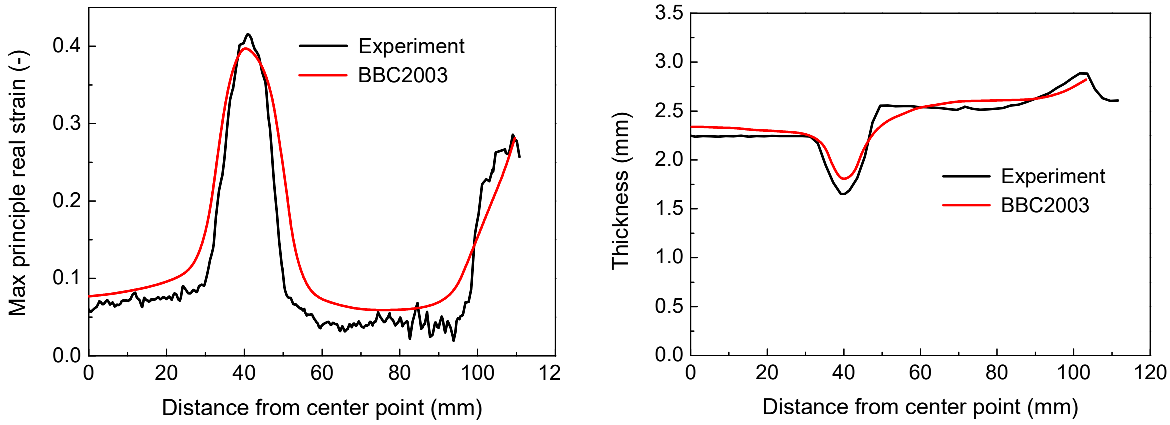

(b) (c)

Fig. 9 Experimental results for gas forming with a complex shape die measured by GOM software. (a) Maximum principal real strain field distribution; (b) Maximum principal real strain and (c) Thickness from the center point to the board

Conclusion

In the presented work, the constitutive behavior of the AA5383 alloy is investigated. A composite model using the BB2003 yield criterion is proposed. The material model is then implemented in a finite element solver to simulate the experimental tests to identify parameters. Uniaxial tension tests are performed at different temperatures, strain rates and for different directions to study the uniaxial tension behavior. Free bulging tests are carried out to characterize the material properties under biaxial stress state. An inverse method is used to obtain the parameters of the BBC2003 yield criterion. It is found that the biaxial yield stress is around 1.3 times of the uniaxial yield stress. The constitutive model is implemented in the user subroutine UMAT by semi-implicit method. The gas forming with a complex shape die is carried out for validation. The results have shown that the composite model with the BBC2003 yield criterion can correctly predict the surface maximum principal logarithmic strain and thickness evolutions. In the future, the damage behavior of the AA5383 alloy in the hot deformation conditions will be considered.

References

[1] R. C. Calcraft, M. A. Wahab, D. M. Viano, G. O. Schumann, R. H. Phillips and N. U. Ahmed, Journal of Materials Processing Technology 92-93 (Supplement C), 60-65 (1999).

[2] H. Conrad, JOM 16 (7), 582-588 (1964).

[3] W. F. Kocks, Progr. Mater. Sci. 19, 291 (1975).

[4] J. H. Sung, J. H. Kim and R. H. Wagoner, International Journal of Plasticity 26 (12), 1746-1771 (2010).

[5] A. S. Khan, Y. Sung Suh and R. Kazmi, International Journal of Plasticity 20 (12), 2233-2248 (2004).

[6] T. Naka, Y. Nakayama, T. Uemori, R. Hino and F. Yoshida, Journal of Materials Processing Technology 140 (1-3), 494-499 (2003).

[7] D. Banabic, International Journal of Plasticity 21 (3), 493-512 (2005).

[8] G. R. Johnson, Proc. 7th Inf. Sympo. Ballistics, 541-547 (1983).

[9] G. Chen, C. Ren, W. Yu, X. Yang and L. Zhang, Proceedings of the Institution of Mechanical Engineers, Part B: Journal of Engineering Manufacture 226 (8), 1287-1297 (2012).

[10] D. Banabic, in Sheet Metal Forming Processes (Springer, 2010), pp. 27-140.
[11] E. M. Taleff, L. G. Hector, R. Verma, P. E. Krajewski and J.-K. Chang, Journal of Materials Engineering and Performance 19 (4), 488-494 (2010).